Journal of King Saud University – Science 34 (2022) 102084

Contents lists available at ScienceDirect

Journal of King Saud University – Science

journal homepage: www.sciencedirect.com

Original article

Facile synthesis of ZnO-NPs from yellow creeping daisy (*Sphagneticola trilobata* L.) attenuates cell proliferation by inducing cellular level apoptosis against colon cancer

Mahadevamurthy Murali [a], S. Manjula [b], N. Shilpa [c], D.K. Ravishankar [d], C.S. Shivakumara [e], Anjana Thampy [e], Abbas Ayeshamariam [f], Sadanand Pandey [g], Satish Anandan [e,*], Kestur Nagaraj Amruthesh [a,*], Fahd A. Al-Mekhlafi [h], K. Kaviyarasu [i,j,*]

[a] *Applied Plant Pathology Laboratory, Department of Studies in Botany, University of Mysore, Manasagangotri, Mysore 570006, Karnataka, India*
[b] *Department of Botany, Government First Grade College, Ramanagara, 562 159, Karnataka, India*
[c] *Department of Studies in Microbiology, University of Mysore, Manasagangotri, Mysore 570006, Karnataka, India*
[d] *Department of Chemistry, Sri Mahadeshwara Government First Grade College, Kollegal 571 440, Karnataka, India*
[e] *Department of Clinical Nutrition and Dietetics, Sri Devaraj Urs Academy of Higher Education and Research, Tamaka, Kolar 563103, Karnataka, India*
[f] *Research Department of Physics, Khadir Mohideen College (Affiliated to Bharathidasan University, Thiruchirappalli), Adirampattinam, 614701, Tamil Nadu, India*
[g] *Department of Chemistry, College of Natural Science, Yeungnam University, 280 Daehak-Ro, Gyeongsan, South Korea*
[h] *Department of Zoology, College of Science, King Saud University, P.O. Box 2455, Riyadh 11451, Saudi Arabia*
[i] *UNESCO-UNISA Africa Chair in Nanosciences/Nanotechnology Laboratories, College of Graduate Studies, University of South Africa (UNISA), Muckleneuk Ridge, PO Box 392, Pretoria, South Africa*
[j] *Nanosciences African Network (NANOAFNET), Materials Research Group (MRG), iThemba LABS-National Research Foundation (NRF), 1 Old Faure Road, 7129, PO Box 722, Somerset West, Western Cape Province, South Africa*

ARTICLE INFO

Article history:
Received 30 January 2022
Revised 28 April 2022
Accepted 9 May 2022
Available online 13 May 2022

Keywords:
Allium cepa
Annexin V staining
Anticancer
MTT assay
Hemolysis

ABSTRACT

Cancer is considered as one of the relatively high mortality diseases to humankind and the search for newer strategies to combat the disease is a never-ending process. In view of the same the present study was designed to biosynthesize zinc oxide nanoparticles (ZnO-NPs) from the aqueous leaf extract (ALE) of medicinally important plant *Sphagneticola trilobata* L. for the first time and to evaluate its efficacy in inducing cancer against HT-29 cells apart from identifying their biocompatible potential. The as-prepared StZnO-NPs were characterized by different techniques that signified the properties of the nanoparticles, which included an absorption peak at 298 nm, bandgap energy of 3.43 eV with a size of ~ 29.83 nm. The scanning electron microscopic images confirmed the particles were agglomerated and the energy dispersive spectroscopic analysis confirmed the particles were of 98.23% purity. The Fourier transform infrared spectroscopy revealed that the metabolites of the ALE act as reducing/ stabilizing agents during the synthesis process which was confirmed by the presence of absorbance peak between 400 cm^{-1} to 600 cm^{-1}. The StZnO-NPs also offered potential antioxidant and genotoxic potential with an IC_{50} value of 0.7 mg mL^{-1}. In addition, the cytotoxic ability of the StZnO-NPs against the HT-29 colon cancer cells and human erythrocytes revealed that the particles were cytotoxic towards HT-29 cells, while insignificant effect against the human erythrocytes. Further, a detailed investigation on the interaction with cells and their inherent toxicity may be enhanced through *in vivo* methods before their therapeutic usage as the StZnO-NPs evaluated during the study offered antioxidant, genotoxic and cytotoxic properties is biocompatible.

* Corresponding authors.
E-mail addresses: satishanandan84@gmail.com (S. Anandan), dr.knamruthesh@botany.uni-mysore.ac.in (K.N. Amruthesh), kavi@tlabs.ac.za (K. Kaviyarasu).

Peer review under responsibility of King Saud University.

Production and hosting by Elsevier

https://doi.org/10.1016/j.jksus.2022.102084

1. Introduction

Nanotechnology is one of the many fields that have brought remarkable development over the 21st century in science and technology and nanomaterials are termed the wonder of modern medicine (Kasinathan et al., 2016; Kaviyarasu et al., 2017; Magdalane et al., 2018). The key to the success of nanotechnology greatly relies on the eco-friendly strategies employed for the development of nanoparticles (Alam, 2021; Bisht and Rayamajhi, 2016; Demchenko, 2012). It is well noted that the conventional methods (physical and chemical) require less time to synthesize bulk amounts of nanoparticles, but the chemicals involved tend to cause toxic implications on the environment (Ansari et al., 2020). Thus, eco-friendly strategies have been developed to overcome the toxic effects of the conventionally developed nanoparticles using biotic sources (plants and microorganisms) as the primary source for synthesizing nanoparticles (Yusof et al., 2019; Murali *et al.,* 2021). Many biological sources employed in the synthesis of nanoparticles, extracts of plant materials (leaf, stem, roots, flowers, etc.) have been extensively used for the synthesis of nanoparticles wherein the active metabolites/enzymes act as reducing and capping agents, thereby helping in the bulk production of the particles which is economically advantageous (Agarwal et al., 2017; Udayshankar et al., 2021). In addition, the usage of plant sources cuts down the potential toxicity of the synthesized particles and can also be produced with the required morphology (size, shape, etc.) (Ahmed et al., 2017; Murali et al., 2021a). Among the metallic and non-metallic nanoparticles, attention has been focused on zinc oxide nanoparticles (ZnO-NPs) due to their broad applications in different fields of science that start from optical to biocontrol to mainly the pharmaceutics due to their stability, non-toxic and cost-effective nature (Mahendra et al., 2020; Lakshmeesha et al., 2020). These nanoparticles have also been "generally recognized as safe" (GRAS) by the US FDA (21CFR182.8991).

The tumor is considered one of the most infectious diseases to humankind, leading to 10 million deaths in 2020. Among the different types of cancer, colon cancer is the third highest in cases reported and stands second in terms of death caused in the last year (2020) (https://www.who.int/news-room/fact-sheets/detail/cancer). Many therapies like chemotherapy, nutrition therapy, stem-cell therapy, targeted drug therapy, gene therapy, etc., have been employed to treat the disease, but an effective treatment/drug is still required for their inhibition has both advantages and disadvantages. Nowadays, the employment of nanoparticles for the inhibition of tumours is gaining importance due to their size and effectiveness (Yao et al., 2020; Murali et al., 2021b). From the literature, it is noted that both metallic and non-metallic nanoparticles have also been employed in the inhibition of tumor cells, including ZnO-NPs (Blanco et al., 2015; Kaviyarasu et al., 2017; Khan et al., 2019; Satish *et al.,* 2019; Murali et al., 2021a). To date, the plant-mediated ZnO-NPs have been known to effectively induce tumors related to the colon, breast, renal, etc., to date (Yao et al., 2020). *Sphagneticola trilobata* L. of the family Asteraceae is a commonly available plant that is widely used for its biopotentialities viz., anti-inflammatory, antioxidant, antimicrobial activities (Lakshmeesha et al., 2020; Mani et al., 2021a; Mani et al., 2021b; Mani et al., 2021c). They also offer wound healing, antihelmintic and anticancer pharmacological activities as it has been noted that the plant is rich in phytoconstituents (such as flavonoids, saponins, phenol, tannins, alkaloids, and cardiac glycosides) and also contains acetylenes and derivatives of kaurenic acid (Sandra et al., 2012; Balekar et al., 2014) and no reports are available to date on the biosynthesis of ZnO-NPs from any of the *Sphagneticola* spp. Due to the strong pharmacological properties of the *Sphagneticola trilobata* L., the synthesis of ZnO-NPs was carried out to evaluate their efficacy in inducing tumor (HT-29 cells) *in vivo,* including antioxidant, genotoxic and biocompatible nature by using human erythrocytes.

2. Materials and methods

2.1. Plant collection, synthesis, and characterization of ZnO-NPs

Healthy leaves of *Sphagneticola trilobata* L. were collected from Mysuru, Karnataka, India. The collected leaves were subjected to extraction with sterile water (1:1) to obtain the extract (ALE). The biosynthesis of ZnO-NPs from the ALE was performed following our previous studies (Murali et al., 2017). The particles obtained (StZnO-NPs) were subjected to the physico-chemical characterization that included UV–Vis spectroscopy [to determine the optical density and bandgap energy by Tauc's equation ($\alpha h\nu$ = D ($h\nu$ - E_g)^n], X-Ray Powder Diffractometer (XRD) (for size and structure), scanning electron microscopic (SEM) analysis (for morphology), Energy Dispersive Spectroscopic (EDS) analysis (for detection of elements) along with Fourier Transform Infrared Spectroscopic (FT-IR) analysis for both ALE and StZnO-NPs to determine the binding properties of biosynthesized nanoparticles using standard procedures.

2.2. Evaluation of biological properties of biosynthesized StZnO-NPs

2.2.1. Antioxidant activity

The radical scavenging activity (RSA) of biosynthesized StZnO-NPs was carried out by the 2,2-diphenyl-1-picrylhydrazyl (DPPH) scavenging method, according to Murali et al. (2020). A range of StZnO-NPs concentrations (0.25–1 mg mL^{-1}) and respective control samples were evaluated for radical scavenging activity using 0.1 mM of DPPH. Each of the selected concentrations of StZnO-NPs was subjected to sonication (15 min) before evaluation. The percent RSA of the nanoparticles was determined by measuring the absorbance using a UV–Vis spectrophotometer.

$$\text{RSA}\,(\%) = \frac{\text{Abs}_{517\text{ nm}}\text{ of Control} - \text{Abs}_{517\text{ nm}}\text{ of Sample}}{\text{Abs}_{517\text{ nm}}\text{ of Control}}\,\text{X}\,100$$

2.2.2. Genotoxic analysis

Allium cepa root tip assay was used to evaluate the genotoxic nature of biosynthesized StZnO-NPs along with respective control. The established roots of healthy onion bulbs were removed and placed upon the glass vials containing sterile distilled water. When the fresh roots reached about 20 to 30 mm long, the onion bulbs were moved to fresh glass vials with the sonicated StZnO-NPs (0.25–1 mg mL^{-1}) samples, which were further subjected to incubation (24 h). The StZnO-NPs treated root tips were carefully cut out and placed in 1 N HCl (2–3 min) for cell wall hydrolysis, followed by repetitive rinses in distilled water. Further, the excised root tips were stained with propidium iodide (nucleic acid-specific staining) (10 mg mL^{-1} in phosphate buffer) for 10 min (Hemanth Kumar et al., 2020) and squashed on a clean glass slide before observing the same under a fluorescence microscope for any chromosomal abnormalities and the percent mitotic index was calculated.

$$\text{Mitotic Index}\,(\%) = \frac{\text{Number of Dividing Cells}}{\text{Total Number of Cells}} \times 100$$

2.3. Cytotoxic analysis

2.3.1. MTT assay of cell inhibition

The anticancer properties of biosynthesized StZnO-NPs were evaluated on HT-29 cell lines procured from NCCS, Pune by 3-(4,

5-dimethylthiazol-2-yl)-2,5-diphenyl tetrazolium bromide (MTT) assay (Selvakumaran et al., 2003). A total of four different concentrations of StZnO-NPs (0.25–1 mg mL^{-1}) were evaluated along with respective control during the study. Each well of the Microtitre plate (96 well plate) was seeded with Dulbecco's modified Eagle's medium (DMEM) (0.1 mL) containing 5×10^5 HT-29 cell suspension and incubated in a humidified atmosphere containing 5% CO_2 for 24 h at 37 °C. The incubated samples were trypsinized/ aspirated, and fresh DMEM (0.1 mL) containing StZnO-NPs and respective control with 10% fetal bovine serum were loaded and incubated at the above-said conditions. The incubated samples were again trypsinized/ aspirated and MTT solution (0.1 mL) prepared in phosphate buffer saline was added to the wells and subjected to incubation for 4 h before their removal and addition of DMSO (0.1 mL) to rapidly solubilize formazan. Further, the optical density of the final samples in the microtitre plates was measured using a Microtitre reader to note the percent cell viability. The experiments were carried out in triplicates.

$$\text{Cell Viability}\,(\%) = \left(\frac{\text{Abs}_{590\,\text{nm}}\ \text{of Sample}}{\text{Abs}_{590\,\text{nm}}\ \text{of Control}}\right) \text{X}\,100$$

2.3.2. Cell cycle analysis

The HT-29 cells were separately seeded in a 6-well plate at a density of 5×10^5 and were cultured in a water-saturated incubation chamber having 5% CO_2 at 37 °C. The growth media was aspirated after the stipulated time and the cells were exposed to St-ZnO-NPs (1 mg) to a final volume of 3 mL $well^{-1}$ for 24 h. At the specified time, the nanoparticle exposed cells were trypsinized and centrifuged for 10 min at 2000 rpm for pellet collection. The cell pellet was fixed with ethanol (0.7 mL) and incubated at −20 °C for 60 min. The fixed cell samples were subjected to washing with ice-cold PBS by centrifugation. The ensuing cell pellet was resuspended in 1 mL of PBS solution containing propidium iodide and RNase A (0.05 g mL^{-1}) and Triton X-100 (0.1%) and incubated for 30 min in the absence of light. The resultant cell suspension was analyzed using a flow cytometer (Cell Lab Quanta™, SC, Beckman Coulter, USA).

2.3.3. Apoptosis/ necrosis analysis

In addition, the St-ZnO-NPs treated HT-29 cells along with control sets as mentioned above were analyzed using Annexin V-FITC staining by using Annexin V-FITC Apoptosis Detection Kit (Invitrogen, USA) as per the manufacturer's instructions. In brief, the StZnO-NPs treated and control HT-29 cells were washed using PBS and resuspended in binding buffer (1X, 0.2 mL). Approximately 0.05 mL of Annexin V-FITC was added to 0.195 mL of cell suspension, thoroughly mixed and subjected to incubation for 10 min at room temperature. At the stipulated time, the cell suspension was washed using the binding buffer (0.2 mL) and resuspended in 0.19 mL of the same buffer and 0.1 mL of propidium iodide was added, mixed thoroughly, incubated for 5 min under the absence of light and analyzed under a flow cytometer.

2.3.4. Cellular morphology assay

The StZnO-NPs treated and control HT-29 cells in DMEM were incubated for 24 h under the absence of light were, trypsinized, centrifuged, washed with ice-cold PBS, and resuspended in PBS. The cell suspension was fixed on glass slides with a coverslip and observed using a Phase contrast microscopy at 20X magnification (Zeiss Axio Vert. A1, Germany).

2.4. Biocompatibility of StZnO-NPs

The biocompatibility of the synthesized StZnO-NPs was evaluated by hemolytic assay (Saraswathi et al., 2017). In concise, about 10 mL blood sample was drawn from healthy volunteers with consent and subjected to centrifugation (3 min at 3000 rpm). The collected erythrocytes were repeatedly washed with Dulbecco's phosphate buffer saline (D-PBS) solution and the final concentration of the resultant sample was adjusted with to D-PBS to get 5% hematocrit (pH 7). The known concentration of StZnO-NPs (0.25–1 mg mL^{-1}) was placed in centrifuge tubes and approximately 3 mL of the erythrocyte suspension was added and mixed gently before incubating at 37 °C for 1 h. The free hemoglobin content in the supernatant was determined by measuring the absorbance at 540 nm using a UV–Vis spectrophotometer.

$$\%\,\text{Haemolysis} = \frac{\text{Absorbance of Test sample} - \text{Absorbance of DPBS}}{\text{Absorbance of 1\% Triton X} - 100 - \text{Absorbance of DPBS}}\,\text{X}\,100$$

2.5. Statistical analysis

The experiments of the study were performed with three replicates and subjected to statistical analysis using SPSS, version 17 (SPSS Inc., Chicago, IL) and the significant differences among the treatment mean values were affirmed by Honestly Significant Difference (HSD) attained by Tukey's test at $p \leq 0.05$ levels.

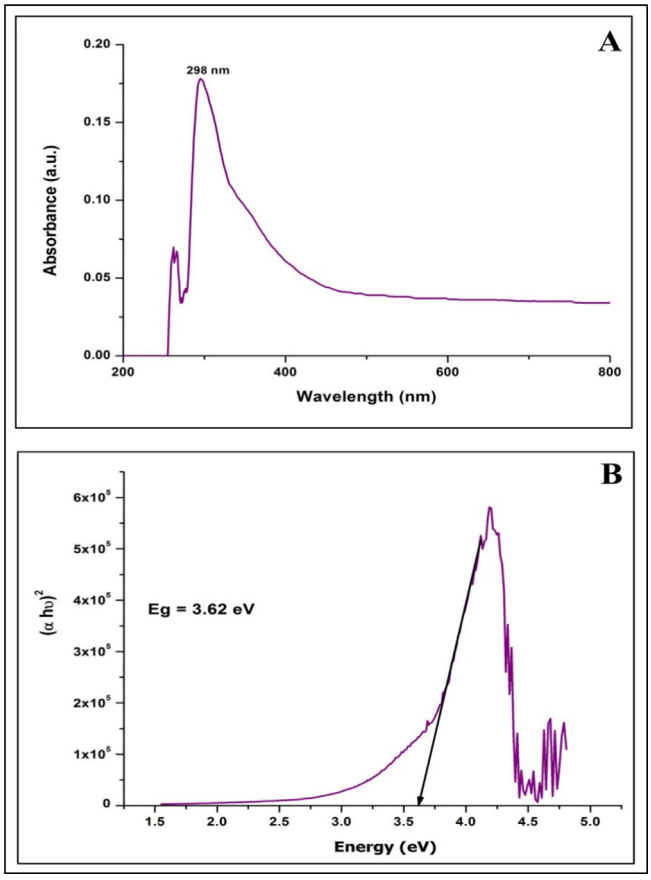

Fig. 1. Ultraviolet–visible spectroscopic analysis (A) and Bandgap energy (B) of biosynthesized StZnO-NPs of *S. trilobata*.

3. Results and discussion

3.1. Plant collection, synthesis, and characterization of ZnO-NPs

The biosynthesized StZnO-NPs were subjected to evaluation for their physico-chemical characters using various techniques. The spectral analysis of the StZnO-NPs evaluated using a spectrophotometer had an absorption peak at 298 nm (Fig. 1A), and the energy bandgap was calculated through Tauc's equation ($\alpha h\nu$ = D ($h\nu$ - E_g)^n was found to be 3.6 eV (Fig. 1B). The obtained results are in affirmation with other studies wherein it is noted that the ZnO-NPs have possessed an absorption peak in long (UV-A) and short wave (UV-B) regions that fall between 280 and 400 nm (Murali et al., 2017; Ansari et al., 2020). In addition to the spectral analysis, it is well noted that the ZnO-NPs have bandgap energy between 3.2 eV and 3.5 eV (Song et al., 2011) and our results also corroborate the findings. Stiff narrow peaks without any notable shift indicate that the crystalline product was observed upon evaluation of StZnO-NPs under XRD, signifying that the particles were pure with a ~ 29.83 nm, which was estimated using Scherrer's formula (Fig. 2A). The stiff narrow peaks were well matched to JCPDS No. 80–510 and in accord with other analyses on ZnO-NPs biosynthesized using plant extracts (Kavya et al., 2020). The absorption of infra-red radiations ALE of the plant at various wavenumbers showed spectrum bands at 3356.13 cm^{-1} [(O–H stretch) Alcohol/phenol group], 1718.78 cm^{-1} [(C = O) esters group], 1634.55 cm^{-1}[(N–H) ester group], 1523.59 cm^{-1} [(N-O) nitro group], 1446.96 cm^{-1} [(C–C) aromatic group], 1367.30 cm^{-1} [(C–H) alkane group] and 655.59 [(-C≡C-H) alkyne group]. In addition, absorbance peak between wavenumber 400 cm^{-1} to 600 cm^{-1} was observed with St-ZnO-NPs and not in the case of ALE which affirms metal oxide bond formation, thereby asserting that the phytoconstituents of the plant extract act as stabilizing and reducing agents during the synthesis of nanoparticles (Fig. 2B). The morphology and elemental analysis of the nanoparticles showed that the biosynthesized particles were agglomerated (Fig. 3A) and of 98.23% purity (Fig. 3B) when analyzed through EDS. Accordingly, from the literature, it may be noted that the physico-chemical characterization through various methods (UV, XRD, SEM, EDS, FT-IR, etc.) is important in identifying the properties of the biosynthesized nanoparticles (Basnet et al., 2018; Kumar et al., 2019).

3.2. Antioxidant activity

The DPPH radical scavenging potentiality of StZnO-NPs evaluated with different concentrations revealed a dose-dependent increase with a half-maximal inhibitory concentration (IC50) of 0.7 mg mL^{-1} (Fig. 4A). The study results specify that the synthesized particles due possess radical scavenging ability and it is a significant factor that helps to inhibit lipid peroxidation and DNA damage within the cells that are directly linked to the complications that arise due to cancer (Lobo et al., 2010). From the available

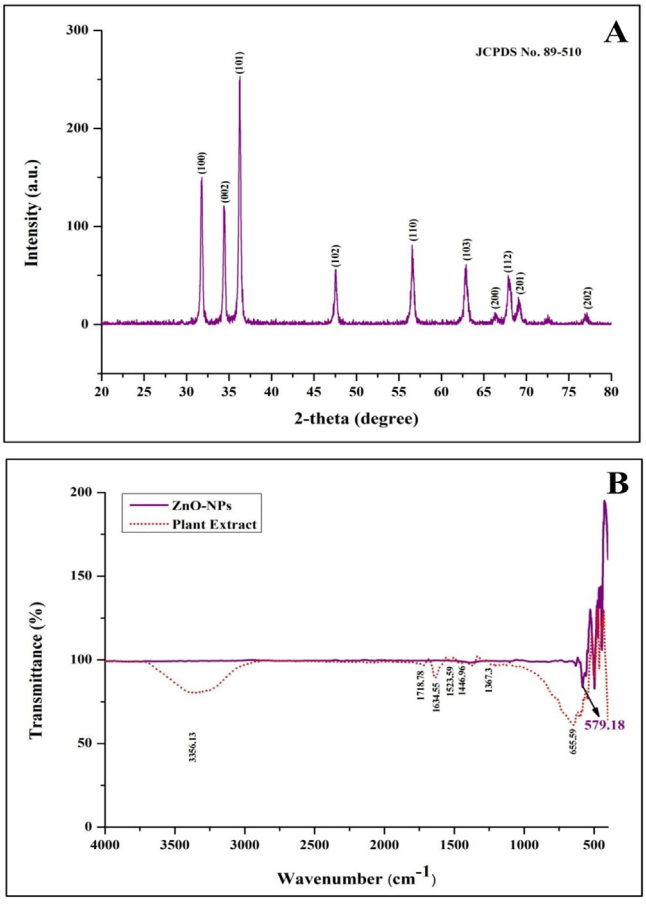

Fig. 2. X-ray diffraction (A) and FTIR spectroscopic analysis of biosynthesized StZnO-NPs of *S. trilobata*.

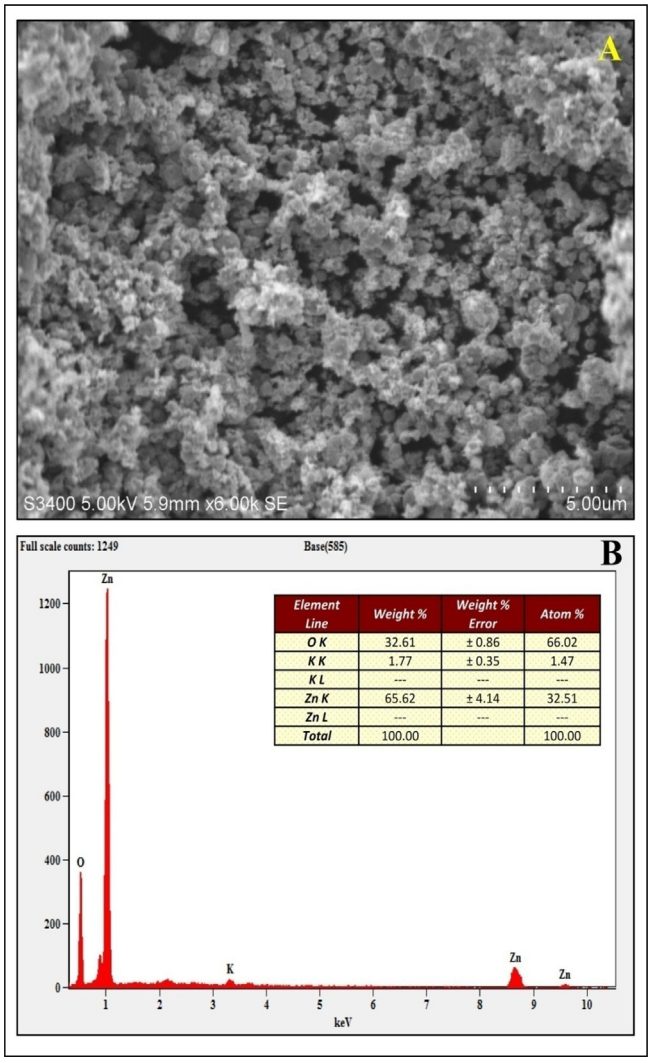

Fig. 3. Scanning Electron Microscopic (A) and EDS (B) analysis of biosynthesized StZnO-NPs of *S. trilobata*.

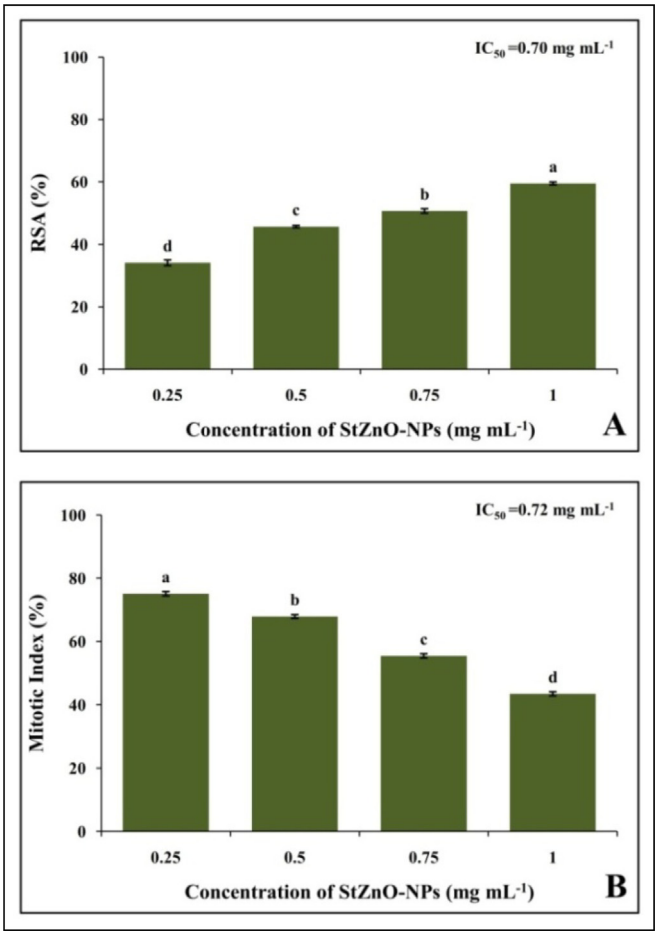

Fig. 4. Representative images of genotoxicity of StZnO-NPs observed in onion root meristem cells.

literature, it is noted that during the synthesis of nanoparticles using biotic agents, the phytoconstituents of the source will act as a possible capping agent that might result in possessing the antioxidant ability of the particles (Basnet et al., 2018; Murali et al., 2021b). In accordance, the synthesis of nanoparticles without using ALE of the plant at the above said concentrations didn't offer significant antioxidant potentiality (data not shown) in the present study.

3.3. Genotoxic analysis

The genotoxicity of the StZnO-NPs was evaluated on onion root tips as the plant species (*Allium cepa*) is identified as a bio-indicator plant by the UN Environmental Programme (UNEP) and the US Environmental Protection Agency (USEPA) (Mesi *et al.,* 2013). The model plant employed in the study is a broadly approved method to evaluate the potential anticancer properties of newer compounds/ metabolites before evaluating the same under *in vitro*, *in vivo* and animal studies along with investigation on factors affecting environmental pollution factors along with toxicity of chemical compounds (Mahendra *et al.,* 2017; Hemanth Kumar et al., 2020; Murali et al., 2021b). The studies noted that the biosynthesized StZnO-NPs could significantly affect the mitosis process within the cells. The synthesized nanoparticles were able to inhibit the mitosis in cells in a concentration-dependent manner with maximum inhibition in the mitotic index of 43.47% at the maximum concentration evaluated with an IC_{50} concentration of 0.72 mg mL^{-1} (Fig. 4B), thereby signifying their efficacy in inhibiting the cell division. It was also noted that the positive (methotrexate) and negative [(sterile distilled water (SDW)] treated root tips mitotic index of 10.36% and 92%, respectively. Also, the microscopic evaluation of StZnO-NPs treated onion root tips upon nuclear staining revealed chromosomal abnormalities in a significant number of cells, while the untreated root tip cells showed usual cell division (Fig. 5). The inhibition in the mitosis process is mainly related to the interaction of the particles with the cells that results in the generation of reactive oxygen species leading to disruption in membrane morphology, electron transport chain and spindle apparatus resulting in DNA damage and cell arrest in mitosis that eventually results in cell apoptosis (Kavya et al., 2020; Murali et al., 2021b). The results of the study denote that the particles possess the ability to inhibit mitosis within the cells leading to apoptosis by signifying their genotoxic potential, which is in conformity with the results of Mahendra *et al.,* (2017) and Heamnath Kumar *et al.,* (2020) in which they noted genotoxic potentiality in plant-based ZnO-NPs upon treatment.

3.4. Cytotoxic analysis

3.4.1. MTT assay of cell inhibition

The cytotoxic efficacy of StZnO-NPs was examined by MTT assay (Rai et al., 2018) on HT-29 cancer cells. The StZnO-NPs revealed a concentration-oriented inhibition against the multiplication of cancer cells after 24 h of treatment, wherein the viability of the cells decreased from 86.46% to 39.42%, with an IC_{50} value of 0.79 mg mL^{-1} (Fig. 6). Nevertheless, the colchicine (standard drug) was used against the HT-29 cell line as a positive control, which offered more than 70% cytotoxicity at 100 μg mL^{-1}. It has been observed that the number of living cells in the culture proportionally represents the total amount of formazan produced due to the activity of mitochondrial dehydrogenase (Kaviyarasu et al., 2017; Magdalane et al., 2018; Murali et al., 2021a). The elevated levels of ROS production damage the DNA of the cells significantly and seize the cell cycle leading to cell death (Singh et al., 2009; Wang et al., 2019). In accordance, the biosynthesized StZnO-NPs offered cytotoxicity towards highly proliferating HT-29 cells due to their ROS production. Our results are consistent with the study reported by Premanathan et al., (2011) wherein ZnO nanoparticles could increase lipid peroxidation in the liposomal membrane by producing reactive oxygen species (ROS). In addition, studies have reported that biosynthesized ZnO nanoparticles from plant extracts have selective and high cytotoxicity towards cancer cells of the colon, glioma, lung, breast, and prostate with less effect on normal cells (Saranya et al., 2017; Amuthavalli et al., 2021; Murali et al., 2021b).

3.4.2. Cell cycle analysis

The cell cycle phase consists of interphases (G1, S, and G2) and mitosis (M) and each phase has its importance in the development of the cell and arresting/ controlling of cell cycle is one of the important approaches in developing anticancer therapeutics (Schwartz et al., 2005). In the study, StZnO-NPs (1 mg mL^{-1}, selected based on maximum percentage cell inhibition in MTT studies) caused G0/G1 cell cycle arrest in the HT-29 cell line, which caused a significant decrease in the accumulation of cells at the S phase after 24 h of treatment (Suppl. Table 2). The cell cycle analysis of untreated cells of the HT-29 cells revealed that 86.48% in G0/G1 phase, 12.03% in S phase and 0.04% in G2 phase, wherein cells treated with StZnO-NPs showed that 90.69%, 7.62% and 1.65% cells in G0/G1 phase, S phase and G2 phase, respectively. The percentage of cells in the G0/G1 phase increased significantly ($p \leq 0.05$) compared to the untreated cells, from 86.48% to 90.69% (Fig. 7). The results suggest that StZnO-NPs arrest at G0/G1phase and the cell population increased, which may be respon-

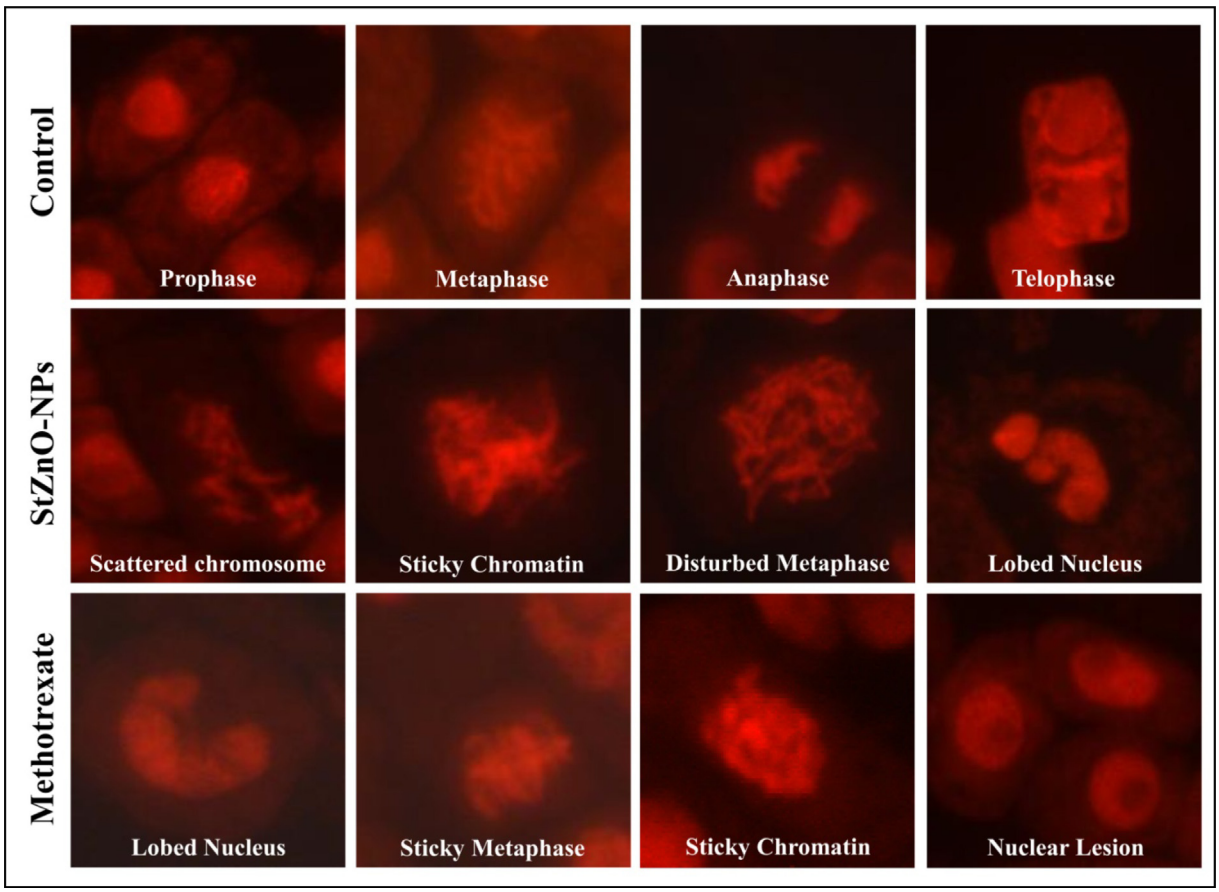

Fig. 5. Representative images of genotoxicity of StZnO-NPs observed in onion root meristem cells.

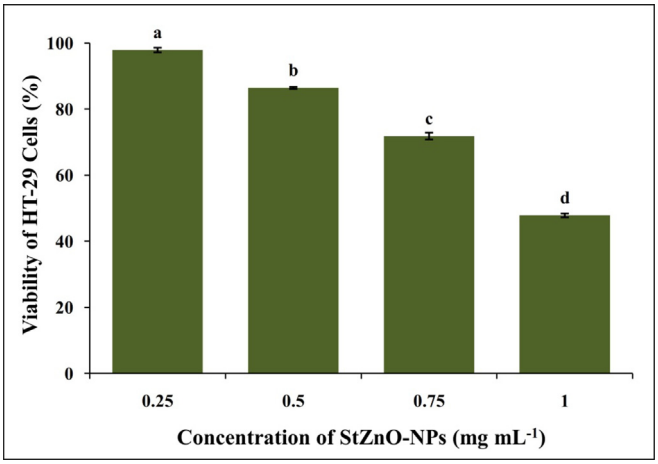

Fig. 6. Effect of StZnO-NPs on HT-29 cells analyzed by MTT assay.

sible for the anti-proliferation of HT-29 cancerous cell line. Further, StZnO-NPs efficacy was comparable to the standard positive control colchicine (320 μg) used in the study. The inhibition process of the cell cycle finally leading to cell death is directly correlated to the generation of oxidative stress upon the interaction of the particles on the cell membrane due to released Zn^{2+} ions (Ramussen *et al.,* 2010; Murali et al., 2021a), which is in confirmation with the results obtained during the present study. In addition, Hanley et al. (2008) have reported that enhanced permeability retention (EPR) and electrostatic interaction properties of biosynthesized particles (ZnO-NPs) towards the cancer cells are preferentially high in the cancer cells compared to normal cells (Rasmussen et al., 2010; Anandan et al., 2019). Further, many studies have indicated that plant-based ZnO-NPs possess cytotoxic potentiality against various cancer-causing cell lines indicating their anticancer properties (Singh et al., 2009; Premanathan et al., 2011; Rai et al., 2018; Wang et al., 2019).

3.4.3. Apoptosis/ necrosis analysis

Annexin-V staining was used to identify early and late apoptosis in StZnO-NPs treated HT-29 cells. It efficiently binds to phosphatidylserine externalized on the outer plasma membrane of apoptotic cells binds to P.S. specifically (Elmore, et al., 2007) and Flow Cytometry was employed to determine the apoptosis caused quantitatively. The presence of P.S. on the cell surface is one of the most important characteristics of apoptosis because of the negative charge phospholipid's potential to change interactions with other lipids that could disrupt the lipid supporting structures (Demchenko, et al., 2012). The HT-29 cells treated with StZnO-NPs induced late apoptotic (82.5%) at 24 h after treatment, whereas colchicine (320 μg) showed an increase in early apoptotic cells (89.06%) (Fig. 8, Suppl. Table 3). Likewise, many studies have reported the cytotoxic potentiality of plant-based ZnO-NPs in cancer-causing cell lines wherein Annexin-V staining was used to detect apoptosis upon treatment (Wang et al., 2019; Murali et al., 2021b). Researchers have demonstrated that, due to the presence of a high percentage of phospholipids as well as specific groups on their surface, cancer cells possess negative zeta potential, which is electrostatically adsorbed by the positively charged zinc oxide nanoparticles (Zn^{2+}), thereby leading to programmed cell death (Guo et al., 2013; Bisht *et al.,* 2016; Wang et al., 2017).

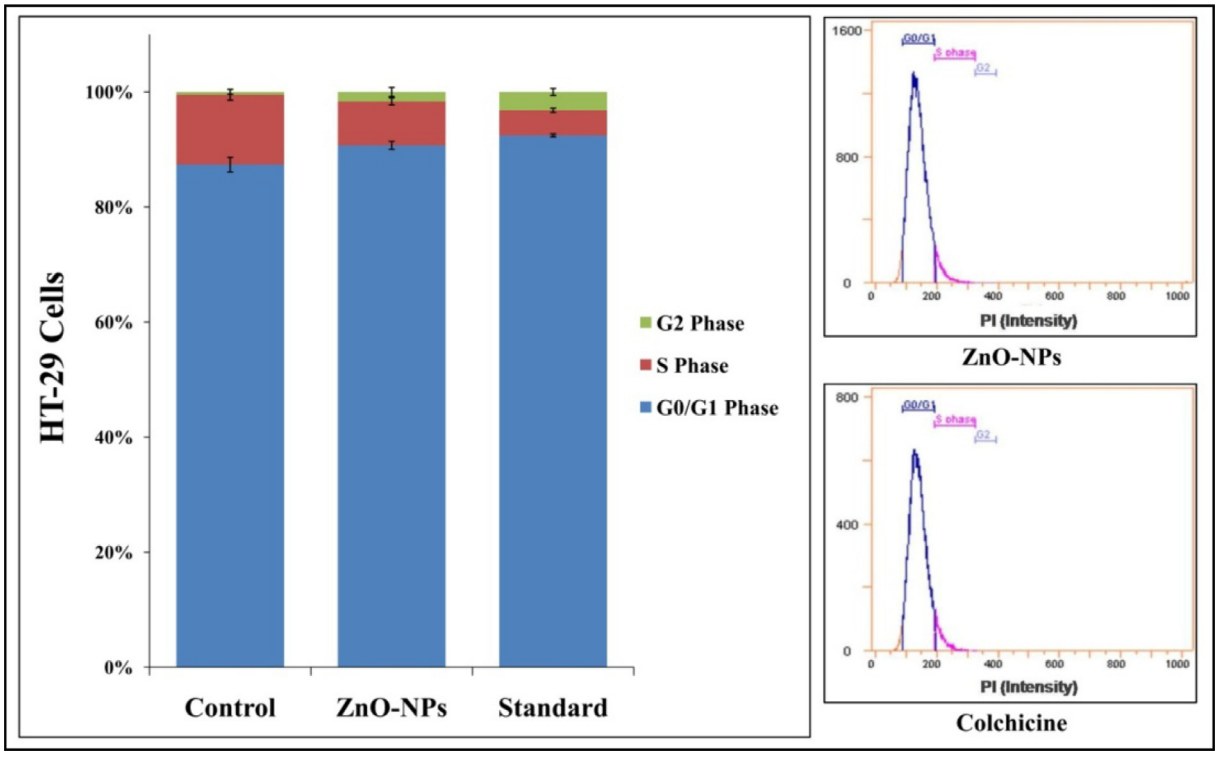

Fig. 7. Cell cycle analysis of StZnO-NPs treated HT-29 cells analyzed on flow cytometry with Annexin-V staining. Each value is the mean of triplicates (n = 3) and vertical bars indicates standard error.

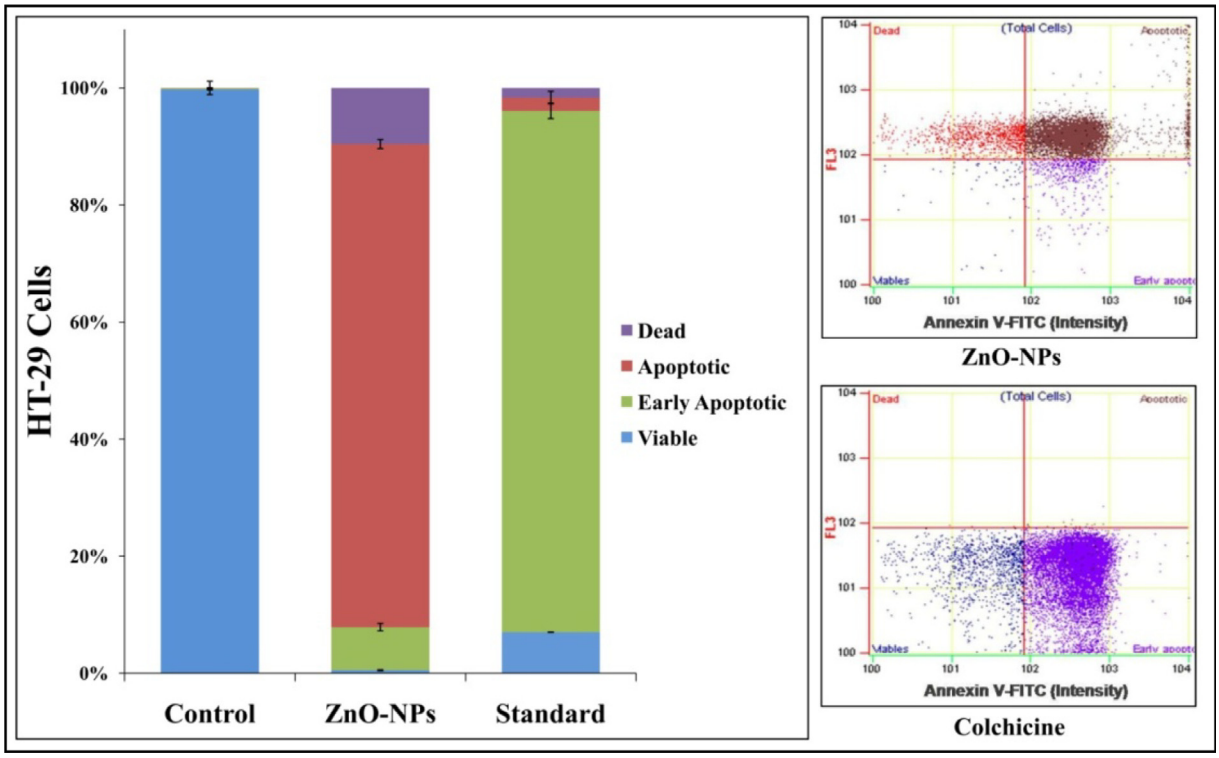

Fig. 8. Apoptotic analysis of StZnO-NPs treated HT-29 cells analyzed on flow cytometry with Annexin-V staining. Each value is the mean of triplicates (n = 3) and vertical bars indicates standard error.

3.4.4. Cellular morphology assay

To validate the results obtained from the above-mentioned cytotoxic analysis, the morphological changes in the cells were conducted. The results showed that the HT-29 cells treated with both StZnO-NPs and colchicine showed morphological changes upon the incubation time that include the formation of apoptotic bodies, membrane blebbing, nuclear fragmentation and shrinkage of cells, which were not observed in control cells (Fig. 9). The

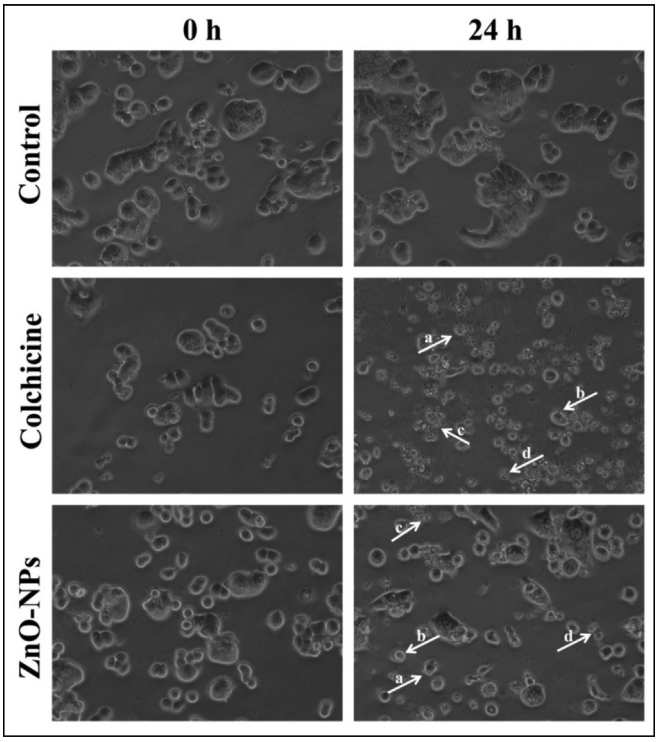

Fig. 9. Representative images of morphological changes observed in HT-29 cells upon treatment with StZnO-NPs. (a) Apoptotic bodies; (b) membrane blebbing; (c) nuclear fragmentation; (d) cellular shrinkage.

changes in the morphological structures of the cell are highly correlated to the interaction of ZnO-NPs with the cancer cells that have resulted in the generation of ROS, leading to the damage to the cell membrane and cellular organelles, including DNA that led to apoptosis (Song et al., 2011; Wang et al., 2015; Vijayakumar et al., 2016).

3.5. Biocompatibility of StZnO-NPs

Given StZnO-NPs potential antioxidant, genotoxic and antitumor properties, it becomes relevant to evaluate its cytotoxic nature against normal cells. The study is mainly based on evaluating the release of hemoglobin from the red blood cells if the tested particles can rupture the cells (Elmore, 2007; Mesi and Kopliku, 2013; Schwartz and Shah, 2005). Hence, we conducted the hemolytic assay against the normal human erythrocytes to confirm its biocompatible nature at different concentrations (0.25–1 mg mL^{-1}) compared to Triton X-100 (1%). The studies observed that the StZnO-NPs offered insignificant hemolysis even at the maximum concentration evaluated (Fig. 10). The haemolytic activity was 1.6% and 4.5% at the minimum and maximum dosage evaluated, whereas Triton X-100 at 1% concentration offered 100% haemolysis. It has been noted that up to 5% hemolysis is regarded as a tolerable limit (Abinaya et al., 2018; Alam et al.,2021).

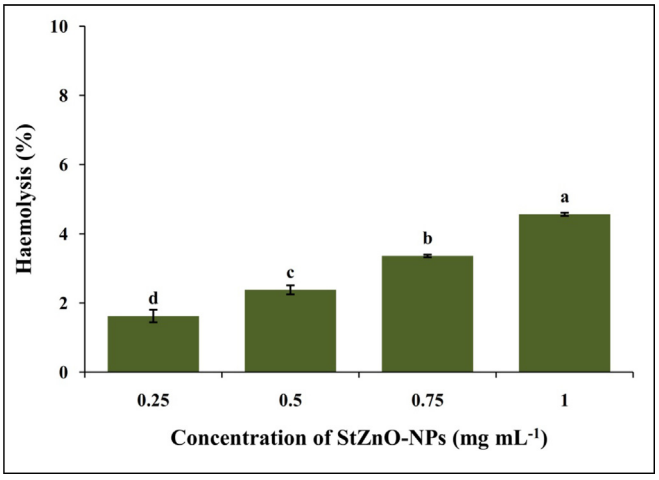

Fig. 10. Biocompatible nature of StZnO-NPs evaluated against the human erythrocytes.

4. Conclusion

The present work reports the first report of the synthesis of ZnO-NPs from the aqueous leaf extract of *Sphagneticola trilobata*. The synthesized StZnO-NPs demonstrated significant antioxidant, genotoxicity (onion root tip method) and cytotoxic properties (HT-29 cells) comparable with that of standard drugs used in the study. In addition, the biocompatible nature of the synthesized StZnO-NPs against the human erythrocytes offered insignificant cytotoxic potential thereby indicating its effectiveness against the cancerous cells. The finding of the study potentiates the efficacy of StZnO-NPs as a good option for the cure of cancer due to its strong antioxidant, genotoxic and cytotoxic properties and safe as they offered no toxicity against the human erythrocytes thereby proving its biocompatible nature.

Declaration of Competing Interest

The authors declare that they have no known competing financial interests or personal relationships that could have appeared to influence the work reported in this paper.

Acknowledgements

The author M.M. would like to thank Department of Studies in Botany, University of Mysore, Mysuru for providing facilities to carry out the research. The corresponding author K.N. Amruthesh would like to thank Govt. of Karnataka VGST-CISEE Programme on “Herbal Drug Technology” for facilities.

References

Abinaya, M., Vaseeharan, B., Divya, M., Sharmili, A., Govindarajan, M., Alharbi, N.S., Kadaikunnan, S., Khaled, J.M., Benelli, G., 2018. Bacterial exopolysaccharide (EPS)-coated ZnO nanoparticles showed high antibiofilm activity and larvicidal toxicity against malaria and Zika virus vectors. J. Trace Elem. Med. Biol. 45, 93–103.

Agarwal, H., Kumar, S.V., Rajeshkumar, S., 2017. A review on green synthesis of zinc oxide nanoparticles–An eco-friendly approach. Resource-Efficient Technologies. 3 (4), 406–413. https://doi.org/10.1016/j.reffit.2017.03.002.

Ahmed, S., Annu, Chaudhry, S.A., Ikram, S., 2017. A review on biogenic synthesis of ZnO nanoparticles using plant extracts and microbes: a prospect towards green chemistry. J. Photochem. Photobiol. B: Biol. 166, 272–284.

Alam, M., 2021. Photocatalytic activity of biogenic zinc oxide nanoparticles: In vitro antimicrobial, biocompatibility, and molecular docking studies. Nanotechnol. Rev. 10 (1), 1079–1091. https://doi.org/10.1515/ntrev-2021-0069.

Amuthavalli, P., Hwang, J.S., Dahms, H.U., Wang, L., Anitha, J., Vasanthakumaran, M., Gandhi, A.D., Murugan, K., Subramaniam, J., Paulpandi, M., Chandramohan, B., Singh, S., 2021. Zinc oxide nanoparticles using plant *Lawsonia inermis* and their mosquitocidal, antimicrobial, anticancer applications showing moderate side effects. Sci. Rep. 11 (1), 1–13. https://doi.org/10.1038/s41598-021-88164-0.

Ansari, M.A., Murali, M., Prasad, D., Alzohairy, M.A., Almatroudi, A., Alomary, M.N., Udayashankar, A.C., Singh, S.B., Asiri, S.M.M., Ashwini, B.S., Gowtham, H.G., Kalegowda, N., Amruthesh, K.N., Lakshmeesha, T.R., Niranjana, S.R., 2020. *Cinnamomum verum* bark extract mediated green synthesis of ZnO nanoparticles and their antibacterial potentiality. Biomolecules. 10, 336. https://doi.org/10.3390/biom10020336.

Balekar, N., Nakpheng, T., Srichana, T., 2014. *Wedelia trilobata* L.: A phytochemical and pharmacological review. Chiang Mai J. Sci. 41 (3), 590–605.

Basnet, P., Chanu, T.I., Samanta, D., Chatterjee, S., 2018. A review on bio-synthesized zinc oxide nanoparticles using plant extracts as reductants and stabilizing agents. J. Photochem. Photobiol. B: Biol. 183, 201–221. https://doi.org/10.1016/j.jphotobiol.2018.04.036.

Bisht, G., Rayamajhi, S., 2016. ZnO nanoparticles: a promising anticancer agent. Nanobiomedicine. 3, 9. https://doi.org/10.5772/63437.
Blanco, E., Shen, H., Ferrari, M., 2015. Principles of nanoparticle design for overcoming biological barriers to drug delivery. Nat. Biotechnol. 33 (9), 941–951. https://doi.org/10.1038/nbt.3330.
Demchenko, A.P., 2012. The change of cellular membranes on apoptosis: fluorescence detection. Exp. Oncol. 34 (3), 263–268. https://doi.org/10.1007/s10616-012-9481-y.
Elmore, S., 2007. Apoptosis: a review of programmed cell death. Toxicol. Pathol. 35 (4), 495–516. https://doi.org/10.1080/01926230701320337.
Guo, D., Bi, H., Liu, B., Wu, Q., Wang, D., Cui, Y., 2013. Reactive oxygen species-induced cytotoxic effects of zinc oxide nanoparticles in rat retinal ganglion cells. Toxicol. In Vitro. 27, 731–738. https://doi.org/10.1016/j.tiv.2012.12.001.
Hanley, C., Layne, J., Punnoose, A., Reddy, K., Coombs, I., Coombs, A., Feris, K., Wingett, D., 2008. Preferential killing of cancer cells and activated human T cells using ZnO nanoparticles. Nanotechnol. 19, (29). https://doi.org/10.1088/0957-4484/19/29/295103 295103.
Hemanth Kumar, N.K., Murali, M., Satish, A., Brijesh Singh, S., Gowtham, H.G., Mahesh, H.M., Lakshmeesha, T.R., Amruthesh, K.N., Jagannath, S., 2020. Bioactive and Biocompatible Nature of Green Synthesized Zinc Oxide Nanoparticles from *Simarouba glauca* DC.: An Endemic Plant to Western Ghats, India. J Clust Sci 31 (2), 523–534.
Kasinathan, K., Kennedy, J., Elayaperumal, M., Henini, M., Malik, M., 2016. Photodegradation of organic pollutants RhB dye using UV simulated sunlight on ceria based TiO2 nanomaterials for antibacterial applications. Sci. Rep. 6 (1), 1–12. https://doi.org/10.1038/srep38064.
Kaviyarasu, K., Geetha, N., Kanimozhi, K., Magdalane, C.M., Sivaranjani, S., Ayeshamariam, A., Kemmedy, J., Maaza, M., 2017. *In vitro* cytotoxicity effect and antibacterial performance of human lung epithelial cells A549 activity of zinc oxide doped TiO2 nanocrystals: investigation of bio-medical application by chemical method. Mater. Sci. Eng. C. 74, 325–333. https://doi.org/10.1016/j.msec.2016.12.024.
Kavya, J.B., Murali, M., Manjula, S., Basavaraj, G.L., Prathibha, M., Jayaramu, S.C., Amruthesh, K.N., 2020. Genotoxic and antibacterial nature of biofabricated zinc oxide nanoparticles from *Sida rhombifolia* Linn. J. Drug Deliv. Sci. Technol. 60,. https://doi.org/10.1016/j.jddst.2020.101982 101982.
Khan, I., Saeed, K., Khan, I., 2019. Nanoparticles: Properties, applications and toxicities. Arab. J. Chem. 12 (7), 908–931. https://doi.org/10.1016/j.arabjc.2017.05.011.
Kumar, N.H., Andia, J.D., Manjunatha, S., Murali, M., Amruthesh, K.N., Jagannath, S., 2019. Antimitotic and DNA-binding potential of biosynthesized ZnO-NPs from leaf extract of *Justicia wynaadensis* (Nees) Heyne-A medicinal herb. Biocatal. Agric. Biotechnol. 18,. https://doi.org/10.1016/j.bcab.2019.101024 101024.
Lakshmeesha, T.R., Murali, M., Ansari, M.A., Udayashankar, A.C., Alzohairy, M.A., Almatroudi, A., Alomary, M.N., Asiri, S.M.M., Ashwini, B.S., Kalagatur, N.K., Nayak, C.S., Niranjana, S.R., 2020. Biofabrication of zinc oxide nanoparticles from *Melia azedarach* and its potential in controlling soybean seed-borne phytopathogenic fungi. Saudi J. Biol. Sci. 27 (8), 1923–1930.
Lobo, V., Patil, A., Phatak, A., Chandra, N., 2010. Free radicals, antioxidants and functional foods: Impact on human health. Pharmacognosy Rev. 4 (8), 118. https://doi.org/10.4103/0973-7847.70902.
Magdalane, C.M., Kaviyarasu, K., Raja, A., Arularasu, M.V., Mola, G.T., Isaev, A.B., Al-Dhabi, N.A., Arasu, M.V., Jeyraj, B., Kennedy, J., Maaza, M., 2018. Photocatalytic decomposition effect of erbium doped cerium oxide nanostructures driven by visible light irradiation: investigation of cytotoxicity, antibacterial growth inhibition using catalyst. J. Photochem. Photobiol. B: Biol. 185, 275–282. https://doi.org/10.1016/j.jphotobiol.2018.06.011.
Mahendra, C., Chandra, M.N., Murali, M., Abhilash, M.R., Singh, S.B., Satish, S., Sudarshana, M.S., 2020. Phyto-fabricated ZnO nanoparticles from *Canthium dicoccum* (L.) for antimicrobial, anti-tuberculosis and antioxidant activity. Process Biochemistry 89, 220–226.
Mani, M., Harikrishnan, R., Purushothaman, P., Pavithra, S., Rajkumar, P., Kumaresan, S., Al Farraj, D.A., Elshikh, M.S., Balamuralikrishnan, B., Kaviyarasu, K., 2021a. Systematic green synthesis of silver oxide nanoparticles for antimicrobial activity. Environ. Res. 202,. https://doi.org/10.1016/j.envres.2021.111627 111627.
Mani, M., Okla, M.K., Selvaraj, S., Ram Kumar, A., Kumaresan, S., Muthukumaran, A., Kaviyarasu, K., 2021b. A novel biogenic *Allium cepa* leaf mediated silver nanoparticles for antimicrobial, antioxidant, and anticancer effects on MCF-7 cell line. Environ. Res. 198,. https://doi.org/10.1016/j.envres.2021.111199 111199.
Mani, M., Pavithra, S., Mohanraj, K., Kumaresan, S., Alotaibi, S.S., Eraqi, M.M., Gandhi, A.D., Babujanarthanam, R., Maaza, M., Kaviyarasu, K., 2021c. Studies on the spectrometric analysis of metallic silver nanoparticles (AgNPs) using *Basella alba* leaf for the antibacterial activities. Environ. Res. 199,. https://doi.org/10.1016/j.envres.2021.111274 111274.
Mesi, A., Kopliku, D., 2013. Cytotoxic and genotoxic potency screening of two pesticides on *Allium cepa* L. Procedia Technol. 8, 19–26. https://doi.org/10.1016/j.protcy.2013.11.005.
Murali, M., Anandan, S., Ansari, M.A., Alzohairy, M.A., Alomary, M.N., Asiri, S.M.M., Almatroudi, A., Thrivveni, M.C., Brijesh Singh, S., Gowtham, H.G., Aiyaz, M., Chandrashekar, S., Urooj, A., Amruthesh, K.N., 2021a. Genotoxic and Cytotoxic properties of zinc oxide nanoparticles phyto-fabricated from the obscure morning glory plant *Ipomoea obscura* (L.) Ker Gawl. Molecules. 26 (4), 891. https://doi.org/10.3390/molecules26040891.
Murali, M., Mahendra, C., Nagabhushan, Rajashekar, N., Sudarshana, M.S., Raveesha, K.A., Amruthesh, K.N., 2017. Antibacterial and antioxidant properties of biosynthesized zinc oxide nanoparticles from *Ceropegia candelabrum* L. – An endemic species. Spectrochimica Acta Part A: Molecular and Biomolecular Spectroscopy 179, 104–109.
Murali, M., Nataraj, K., Gowtham, H.G., Ansari, M.A., Alomary, M.N., Alghamdi, S., Shilpa, N., Singh, S.B., Thriveni, M.C., Aiyaz, M., Nataraju, A., Lakshmidevi, N., Adil, S.F., Hatshan, M.R., Amruthesh, K.N., 2021b. Plant-Mediated Zinc Oxide Nanoparticles: Advances in the New Millennium towards Understanding Their Therapeutic Role in Biomedical Applications. Pharmaceutics. 13 (10), 1662. https://doi.org/10.3390/pharmaceutics13101662.
Premanathan, M., Karthikeyan, K., Jeyasubramanian, K., Manivannan, G., 2011. Selective toxicity of ZnO nanoparticles toward Gram-positive bacteria and cancer cells by apoptosis through lipid peroxidation. Nanomed.: Nanotechnol. Biol. Med. 7 (2), 184–192. https://doi.org/10.1016/j.nano.2010.10.001.
Rai, Y., Pathak, R., Kumari, N., Sah, D.K., Pandey, S., Kalra, N., Soni, R., Dwarakanath, B.S., Bhatt, A.N., 2018. Mitochondrial biogenesis and metabolic hyperactivation limits the application of MTT assay in the estimation of radiation induced growth inhibition. Sci Rep 8 (1).
Rasmussen, J.W., Martinez, E., Louka, P., Wingett, D.G., 2010. Zinc oxide nanoparticles for selective destruction of tumor cells and potential for drug delivery applications. Expert Opin. Drug Deliv. 7 (9), 1063–1077. https://doi.org/10.1517/17425247.2010.502560.
Sandra, S.M., Nilton, S.A., Sergio, R.A., Ana, C.Z., Rubia, C., Thiago, M.C., Sergio, H.F., Fernando, Q.C., Waldiceu Jr., A.V., 2012. Kaurenoic acid from *Sphagneticola trilobata* inhibits inflammatory pain: effect on cytokine production and activation of the NO–cyclic GMP–protein kinase G-ATP-sensitive potassium channel signaling pathway. J. Nat. Prod. 75, 896–904. https://doi.org/10.1021/np200989t.
Saranya, S., Vijayaranai, K., Pavithra, S., Raihana, N., Kumanan, K., 2017. *In vitro* cytotoxicity of zinc oxide, iron oxide and copper nanopowders prepared by green synthesis. Toxicol. Rep. 4, 427–430. https://doi.org/10.1016/j.toxrep.2017.07.005.
Saraswathi, V.S., Tatsugi, J., Shin, P.K., Santhakumar, K., 2017. Facile biosynthesis, characterization, and solar assisted photocatalytic effect of ZnO nanoparticles mediated by leaves of *L. speciosa*. J. Photochem. Photobiol. B: Biol. 167, 89–98. https://doi.org/10.1016/j.jphotobiol.2016.12.032.
Anandan, S., Mahadevamurthy, M., Ansari, M.A., Alzohairy, M.A., Alomary, M.N., Farha Siraj, S., Halugudde Nagaraja, S., Chikkamadaiah, M., Thimappa Ramachandrappa, L., Naguvanahalli Krishnappa, H.K., Ledesma, A.E., Nagaraj, A.K., Urooj, A., 2019. Biosynthesized ZnO-NPs from *Morus indica* attenuates methylglyoxal-induced protein glycation and RBC damage: *In-vitro*, *in-vivo* and molecular docking study. Biomolecules. 9 (12), 882.
Schwartz, G.K., Shah, M.A., 2005. Targeting the cell cycle: A new approach to cancer therapy. J. Clin. Oncol. 23 (36), 9408–9421. https://doi.org/10.1200/JCO.2005.01.5594.
Selvakumaran, M., Pisarcik, D.A., Bao, R., Yeung, A.T., Hamilton, T.C., 2003. Enhanced cisplatin cytotoxicity by disturbing the nucleotide excision repair pathway in ovarian cancer cell lines. Cancer Res. 63, 1311–1316.
Singh, N., Manshian, B., Jenkins, G.J.S., Griffiths, S.M., Williams, P.M., Maffeis, T.G.G., Wright, C.J., Doak, S.H., 2009. NanoGenotoxicology: the DNA damaging potential of engineered nanomaterials? Biomaterials. 30 (23-24), 3891–3914.
Song, Z., Kelf, T.A., Sanchez, W.H., Roberts, M.S., Ricka, J., Frenz, M., Zvyagin, A.V., 2011. Characterization of optical properties of ZnO nanoparticles for quantitative imaging of transdermal transport. Biomed. Opt. Express. 2 (12), 3321–3333. https://doi.org/10.1364/BOE.2.003321.
Udayshankar, A.C., Shivaram, A.B., Murali, M., Lakshmeesha, T.R., Lalitha, S.G., Hemanth Kumar, N.K., Satish, A., Brijesh, S.S., Eswaraiah, G.C., Niranjana, S.R., 2021. Biosynthesis of zinc oxide nanoparticles using leaf extract of *Passiflora subpeltata*: Characterization and Antibacterial activity against *Escherichia coli* isolated from poultry faeces. J. Clust. Sci. 32, 1663–1672. https://doi.org/10.1007/s10876-020-01926-0.
Vijayakumar, S., Vaseeharan, B., Malaikozhundan, B., Shobiya, M., 2016. *Laurus nobilis* leaf extract mediated green synthesis of ZnO nanoparticles: Characterization and biomedical applications. Biomed. Pharmacother. 84, 1213–1222. https://doi.org/10.1016/j.biopha.2016.10.038.
C. Wang X. Hu Y. Gao Y. Ji ZnO Nanoparticles Treatment Induces Apoptosis by increasing intracellular ROS Levels in LTEP-a-2 Cells BioMed Res. Int. 2015 2015 1 9 423287.
Wang, J., Lee, J.S., Kim, D., Zhu, L., 2017. Exploration of zinc oxide nanoparticles as a multitarget and multi-functional anticancer nanomedicine. ACS Appl. Mater. Interfaces. 9 (46), 39971–39984. https://doi.org/10.1021/acsami.7b11219.
Wang, Y., Zhang, Y., Guo, Y., Lu, J., Veeraraghavan, V.P., Mohan, S.K., Wang, C., Yu, X., 2019. Synthesis of zinc oxide nanoparticles from *Marsdenia tenacissima* inhibits the cell proliferation and induces apoptosis in laryngeal cancer cells (Hep-2). J. Photochem. Photobiol. B: Biol. 201,. https://doi.org/10.1016/j.jphotobiol.2019.111624 111624.
Yao, Y., Zhou, Y., Liu, L., Xu, Y., Chen, Q., Wang, Y., Wu, S., Deng, Y., Zhang, J., Shao, A., 2020. Nanoparticle-based drug delivery in cancer therapy and its role in overcoming drug resistance. Front. Mol. Biosci. 2020, 7. https://doi.org/10.3389/fmolb.2020.00193.
Yusof, H.M., Mohamad, R., Zaidan, U.H., 2019. Microbial synthesis of zinc oxide nanoparticles and their potential application as an antimicrobial agent and a feed supplement in animal industry: A review. J. Ani. Sci. Biotechnol. 10 (1), 1–22. https://doi.org/10.1186/s40104-019-0368-z.